Investigating the impacts of aerodynamics of wings and body on airplane motion equations

Mohammad Reza HASSANNEZHAD

B.Sc. of Aeromechanic Technology Engineering,
Aviation Services and Technology University of Applied Science of Mashhad, Iran

Reza.succes@gmail.com

Abstract: In this project, the effect of aircraft body flexibility in aerodynamic mode was studied. In the second section, assuming creation of bending in the body by horizontal and vertical tails, the longitudinal and transverse stability derivatives of the aircraft were obtained and, as shown, body flexibility reduced stability of the aircraft and also reduced power of tail control surfaces. This decrease increases with increasing speed such that these effects are noticeable at higher speeds. In the next section, natural frequencies of aircraft structure were obtained by discretization of continuous masses into discrete concentrated masses, and as observed, as the number of masses increased, the obtained results became more accurate and converged toward real value. However, if the plane is subjected to unplanned maneuver of plunging in critical conditions and given the fact that the aircraft has not been designed for such maneuvers, the impact of body flexibility in such conditions would be significant, that as was observed, through aerodynamic considerations and ABAQUS software outputs, airplanes can achieve complete safety. After aerodynamic examination of flight of elastic airplanes, the issue of controlling these planes can be considered. For this purpose, it is necessary to obtain airplane conversion function with regard to flexibility of the structure. In this case, the zeros and poles of elastic airplane conversion function will be different from stiff state and require specific measures.

Keywords: aerodynamics, airplane, optimization, elastic, mass concentration.

1. Introduction

In common flight mechanics references and books, the equations of aircraft motion are generally obtained by assuming stiffness of aircraft structure, and the impacts of flexibility of structure are not considered. In cases where natural frequencies of aircraft aerodynamics, assuming stiffness, are significantly different from natural vibrational frequencies of structure, stiffness assumption in order for aerodynamic analysis of the aircraft will be consistent with reality to an acceptable extent. But as flexibility of structure increases and natural vibrational frequencies of structure decrease, this difference is reduced and the assumption of structure stiffness will no longer be acceptable (Chernyshev et al., 2019). This has caused experts in the field to take into account flexibility of structure in obtaining aircraft motion equations. With the development of larger aircrafts with long body and much wider wing span in the 1950s, as well as the use of jet engines and increased aircraft speed, numerous problems arose and some of them led to fatal accidents. Also, use of new alloys and newly emerging composites in the following years led to dramatic increase of flexibility of structure, such that not taking into account the flexibility of structure in large subsonic and speed of sound aircrafts as well as supersonic fighter planes not only reduced accuracy of analysis, but also provided completely false results to analysts. In fact, flight aerodynamic modes and structure vibrational modes are coupled together (Cui et al, 2018). But this dependency is typically much lower in small and low-speed aircrafts in comparison with large and high-speed aircrafts, as in small and low-speed aircrafts the natural frequency of longitudinal and latitudinal flight modes, including Short Period, Long Period, Roll, Duch-roll, and Spiral, are much less than natural vibrational frequencies of structure; such that the dependency of flight and vibration modes of the structure can be neglected and not taking into account flexibility of structure does not cause any significant error (Du & Tang, 2018).

Table 1 compares the lowest natural frequencies of some aircrafts (Guttag & Reis, 2017). It is observed that in planes such as Concord, B-1 and C-5, the lowest natural frequency is in the

https://doi.org/10.33436/v30i4y202004

range between 11 and 13 radians per second. Therefore, it is necessary to determine the effects of structure flexibility on aircraft aerodynamics. This is discussed in the following sections in detail.

Table 1. The lowest natural vibrational frequency of some different aircraft types

Aircraft name	Aircraft type	Natural frequency *rad/sec*
B-1	Supersonic Bomber	13
Concord	Supersonic Passenger	13
C-5	Heavy Transport	11
Airbus 380	Heavy Passenger	6.25

2. Materials and methods

Motion equations of six degrees of freedom of elastic airplane

The method for finding the simplest mathematical model for elastic aircraft in order for aerodynamic flight analysis and control system design has always been one of the most important issues discussed in aerodynamics of flying objects. Considering the issues discussed in the previous section, taking into account flexibility of structure is so much crucial in designing next-generation aircrafts. Reduced weight of structure, lack of aerodynamic stability, and use of very complex feedback control systems lead to reduction of frequency distances of flight modes of stiff aircraft and frequency of vibrating modes. In addition, the ability to apply control systems with the ability of reshaping the structure requires careful modeling of the flying object taking into account structure flexibility. Therefore, it is especially important to investigate the effects of structure flexibility on aircraft flight responses, which requires integrating aircraft's motion and vibration equations. Obtaining motion equations of elastic airplane has been studied by Heinz (2017), Ideen (2020), Li et al. (2020), Naveen (2018). Stalewski, & Żółtak (2012), and Tuzcu (2016) have investigated the coupling between stiff aircraft modes and elastic modes. Warren Woodrow (2013) simulated flight of elastic airplane. This study showed that increasing flexibility of structure even to a moderate extent, negative effects on quality of aircraft direction will be created.

Obtaining motion equations of elastic airplane

In this section a continuous model for aircraft including motion and vibration equations of structure is presented (Xianhong et al., 2017). Motion equations of aircraft in body device will be obtained. In this case, the obtained model can be used for various flight simulations. It is necessary to make some assumptions in order to achieve this goal. By considering structural deformations to be small (first hypothesis), linear elastic theory can be used. It is also assumed that natural vibrational frequencies of structure as well as form of modes have been obtained using methods such as Finite Element or other methods (second hypothesis). In this case, using Lagrange equation directly results in obtaining motion equations as ordinary differential equations expressed in terms of generalized forces along with aerodynamic and propulsion forces. The degrees of stiff and elastic freedom of aircraft are eventually coupled together by these forces. In order to express the generalized aerodynamic forces in terms of form of modes, forces, and aerodynamic moments, integral expressions will be obtained. Using Aerodynamic Strip Theory, analytical expressions for aerodynamic forces and moments are obtained. Use of Aerodynamic Strip Theory does not mean priority of this method over other methods; rather, some coefficients can be obtained by practical methods or numerical methods. In case of invention of better methods in this regard, the existing methods can be replaced by them. However, use of Aerodynamic Strip Theory has two advantages. In the early stages of design and when accurate information about final design is not available, this method can provide relatively acceptable responses for high aspect ratios. Also, importance of this method is evident as it results in obtaining analytical expressions that, compared to numerical results, provide a better view to designers.

Aerodynamics of unconstrained elastic object

The position of a mass element ρdv of an elastic object in inertial coordinate system $\mathbf{OXYZ}$ can be considered based on the position of that element in a local device ($\mathbf{oxyz}$) and the local device coordinates relative to inertial coordinates ($\mathbf{OXYZ}$) as shown in Figure (1), such that $\overline{R} = \overline{R}_0 + \overline{\rho}$. Then, kinetic energy of the whole object will be:

$$T = \frac{1}{2}\int_V \frac{d\,\overline{R}}{dt} \cdot \frac{d\,\overline{R}}{dt}\rho \mathbf{dV} \tag{1}$$

If the local coordinate system $\mathbf{oxyz}$ rotates at an angular velocity of ω relative to the inertial coordinate system $\mathbf{OXYZ}$, and each of mass elements are considered as point masses (simplifying assumption 3), then:

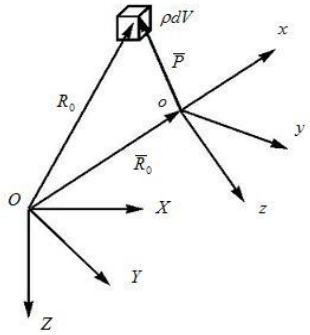

Figure 1. Position of mass element

$$\frac{d\,\overline{R}}{dt} = \frac{d\,\overline{R}_0}{dt} + \frac{\delta\,\overline{P}}{\delta t} + \overline{\omega} \times \overline{p} \tag{2}$$

Where $\frac{\delta\,\overline{P}}{\delta t}$ represents $\overline{p}$ derivative relative to time in local device.

In this case, kinetic energy of the whole object will be equal to:

$$T = \frac{1}{2}\int_V \left\{ \frac{d\,\overline{R}_0}{dt} \cdot \frac{d\,\overline{R}_0}{dt} + 2\frac{d\,\overline{R}_0}{dt} \cdot \frac{\delta\,\overline{p}}{\delta t} + \frac{\delta\,\overline{p}}{\delta t} \cdot \frac{\delta\,\overline{p}}{\delta t} + \right.$$

$$\left. 2\frac{\delta\,\overline{p}}{\delta t} \cdot (\overline{\omega} \times \overline{p}) + (\overline{\omega} \times \overline{p}) \cdot (\overline{\omega} \times \overline{p}) + 2(\overline{\omega} \times \overline{p}) \cdot \frac{d\,\overline{R}_0}{dt} \right\} \rho \, \mathrm{dV} \tag{3}$$

Potential energy of object includes elastic strain energy and potential energy resulted from gravity. Potential energy resulted from gravity is equal to:

$$U_g = -\int_V \overline{g} \cdot (\overline{R}_0 + \overline{p}) \rho \, \mathrm{dV} \tag{4}$$

Where, $\overline{g}$ represents gravity acceleration vector. Elastic strain energy resulted from object deformation is equal to the work done to cause the deformation in the object. If position of a point of the object is stated based on its position before deformation, $\overline{s}(x, y, z)$, plus the displacement caused by deformation, $\overline{d}(x, y, z, t)$, then the position of each element will be equal to:

$$\overline{p} = \overline{s} + \overline{d} \tag{5}$$

According to D'Alembert's Principle, strain energy is equal to:

$$U_e = -\frac{1}{2}\int_V \frac{\delta^2 \bar{d}}{\delta t^2}\cdot \bar{d}\rho \, \mathrm{dV} \tag{6}$$

Determination of aerodynamic forces

Now the aerodynamic forces must be determined. For this purpose, the aerodynamic forces and moments must be examined individually.

Determination of lift and moment forces of the torsion resulted from bending and torsional vibration of the wing:

One way to determine aerodynamic forces is to use strip theory. The underlying assumption of this theory is that lift aerodynamic force l (per unit width of wing) on a two-dimensional airfoil depends on angle of attack of the airfoil cross section α_s.

$$l = \frac{1}{2}\rho V_{0^2} c C_{l\alpha}\alpha_s \tag{7}$$

So, total lift force for the aircraft is expressed as below:

$$L = L_{fuselage} + \int_{-\frac{b}{2}}^{+\frac{b}{2}} l_{wing}\, dy + \int_{-\frac{bt}{2}}^{+\frac{bt}{2}} l_{tail}\, dy \tag{8}$$

To illustrate application of strip theory for elastic aircraft and simplification, a straight wing (without backwardness) with opening of b according to Figure 2 is considered. According to geometry of the cross section as well as the effect of vibration on deformation of wing, the angle of attack of cross section can be estimated as below:

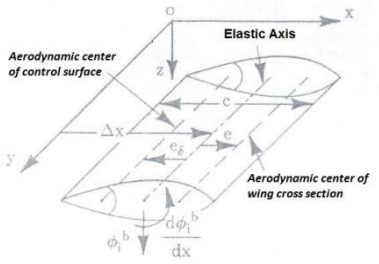

Figure 2. Wing cross section

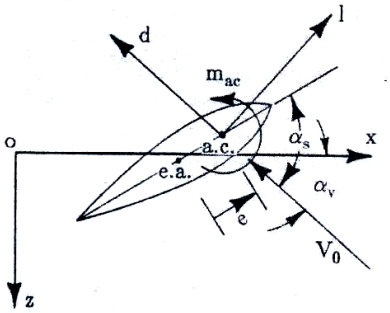

Figure 3. Two-dimensional cross section of wing

$$\alpha_s = \alpha_v + i_s - q\left(\frac{\Delta x + e}{U}\right) + p\frac{y}{U} + \sum_{i=1}^{\infty}\left[\left(\frac{d\varphi_i^b}{dx}\right)\eta_i + \frac{1}{U}\varphi_i^b\dot{\eta}_i\right] \tag{9}$$

Where, $\alpha_v \triangleq \tan^{-1}[W/U]$ is equal to angle of attack of the aircraft, i_s is angle of wing installation, φ_i^b is displacement resulted from wing bending in line with **z** due to i-mode, and $d\varphi_i^b/dx$ is torsional displacement of cross section due to i-mode assuming no change in shape of the cross-section.

By placing angle of attack from the above equation in equation (10), the following equation for lift force of the whole wing is obtained:

$$L_w = \frac{\rho V_0^2 S}{2}\left[C_{L0} + C_{L\alpha}\alpha_v + C_{Lp}\rho + C_{Lq}q + C_{L\delta}\delta + \sum_{i=1}^{\infty}(C_{L\eta i}\eta_i + C_{L\dot{\eta} i}\dot{\eta}_i)\right] \quad (10)$$

In this example, a straight wing with no angle of backwardness has been examined and down wash effects have also been ignored. The coefficients related to $\dot{\alpha}$ were also not considered. However, these terms can also be considered.

For torsional moment, *M*, also using a similar procedure, a similar equation can be obtained.

$$\underline{M} = \frac{\rho V_0^2 S\bar{c}}{2}\left[C_{M0} + C_{M\alpha}\alpha_v + C_{Mp}p + C_{Mq}q + C_{M\delta}\delta + \sum_{i=1}^{\infty}(C_{M\eta i}\eta_i + C_{M\dot{\eta} i}\dot{\eta}_i)\right] \quad (11)$$

Not considering the effects of cross section drag, all the coefficients of equations (12) and (13) can be obtained. These coefficients are shown in Table 2. The coefficients related to other forces and moments are obtained similarly. A similar procedure is used to determine the generalized forces for elastic degrees of freedom. Figure 3 shows the forces and moments applied to a wing cross section. In the figure, two degrees of elastic freedom have been considered for bending and torsion of the wing. So, the work done for the whole elastic deformations is equal to the sum of the work done to create the bending and the work done to create the torsion. Not considering the drag force we will have:

$$W_{bend} = -l\cos\alpha_v \sum_{i=1}^{\infty}\varphi_{ib}\eta_h^2 \quad (12)$$

$$W_{torsion} = (m_{ac} + le\cos\alpha_v)\sum_{i=1}^{\infty}\left(\frac{d\varphi_{idx}^b}{dx}\right)\eta_i \quad (13)$$

So, the generalized forces for degrees of elastic freedom are obtained as below:

$$Q_{\eta i} = \int_{-\frac{b}{2}}^{+\frac{b}{2}}\left\{(-l\cos\alpha_v\varphi_i^b) + \left[(m_{ac} + le\cos\alpha_v)\sum_{i=1}^{\infty}\left(\frac{d\varphi_i^b}{dx}\right)\right]\right\}\mathrm{dy} \quad (14)$$

Assuming $\cos\alpha_s = \cos\alpha_v$ equation 15 can be estimated as below:

$$Q_{\eta i} = (A_i + B_i)\cos\alpha_v + C_i \quad (15)$$

$$A_i = -\int_{-\frac{b}{2}}^{+\frac{b}{2}} l\varphi_i^b\,\mathrm{dy} \qquad B_i = -\int_{-\frac{b}{2}}^{+\frac{b}{2}} le\left(\frac{d\varphi_i^b}{dx}\right)\mathrm{dy} \qquad C_i = -\int_{-\frac{b}{2}}^{+\frac{b}{2}} m_{ac}\left(\frac{d\varphi_i^b}{dx}\right)\mathrm{dy} \quad (16)$$

The coefficients of generalized forces for degrees of elastic freedom, equations 17 and 18, can be expressed as aerodynamic coefficients. For example:

$$A_i = \frac{\rho V_0^2 S\bar{c}}{2}\left[C_0^{Ai} + C_\alpha^{Ai}\alpha_v + C_p^{Ai}p + C_q^{Ai}q + C_\delta^{Ai}\delta + \sum_{i=1}^{\infty}(C_{\eta h}^{Ai}\eta_i + C_{\dot{\eta} h}^{Ai}\dot{\eta}_i)\right] \quad (17)$$

Other coefficients related to generalized forces of B_i and C_i can be defined similarly. By combining all the coefficients related to generalize forces, the general coefficients are obtained. For example, by expanding coefficients of forces, the following equation is obtained:

$$Q_{\eta i} = \frac{\rho V_0^2 S\bar{c}}{2}\{\ [(C_0^{Ai} + C_0^{Bi}) + (C_\alpha^{Ai} + C_\alpha^{Bi})\alpha_v + (C_p^{Ai} + C_p^{Bi})p + (C_q^{Ai} + C_q^{Bi})q + (C_\delta^{Ai} + C_\delta^{Bi})\delta + \sum_{i=1}^{\infty}(C_{\eta h}^{Ai} + C_{\eta h}^{Ai})\eta_i \sum_{i=1}^{\infty}(C_{\eta h}^{Ai} + C_{\eta h}^{Ai})\dot{\eta}_i]\cos\alpha_v + [C_0^{Ai} + C_\alpha^{Ai}\alpha_v + C_p^{Ai}p + C_q^{Ai}q + C_\delta^{Ai}\delta + \sum_{i=1}^{\infty}(C_{\eta h}^{Ai} + C_{\eta h}^{Ai}\dot{\eta}_i)]\ \} \quad (18)$$

By arranging equation 19, the following equation is obtained:

$$Q_{\eta i} = \frac{\rho V_0^2 S\bar{c}}{2}\left[C_0^{\eta i} + C_\alpha^{\eta i}\alpha_v + C_\delta^{\eta i}\delta + \sum_{i=1}^{\infty} C_{\eta i}^{\eta i}\eta_i + C_p^{Ai}p + C_q^{Ai}q + \sum C_{\dot{\eta} i}^{\eta i}\dot{\eta}_i\right] \quad (19)$$

Obtaining motion equations of concentrated masses

Now, this method is described in the form of a simple example for wing of the plane (Tuzcu, 2016). In this method, using Lagrange equation, motion equation of concentrated masses is obtained and then using the obtained equations, natural frequencies and shape of modes are obtained. To use Lagrange equation, kinetic energy and potential energy of each concentrated mass must be calculated.

$$\frac{d}{dT}\left(\frac{\partial T}{\partial \dot{q}_j}\right) - \frac{\partial T}{\partial q_j} + \frac{\partial F}{\partial \dot{q}_j} + \frac{\partial U}{\partial q_j} = Q \quad (20)$$

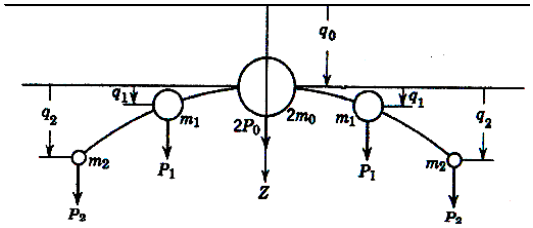

Figure 4. Discrete mass of aircraft wing

In the forces shown in Figure 4, P_i s represent the forces exerted on each of the discrete masses that here, these forces include the forces caused by gravity as well as aerodynamic forces. These forces are combined together and are exerted in Lagrange equation as generalized forces, *Q*. It should be noted that due to symmetry of the system, only one wing is considered for analysis.

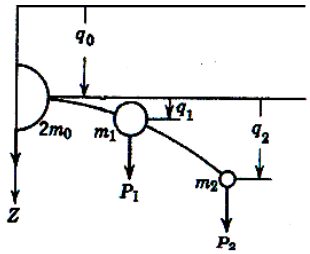

Figure 5. Discrete mass model for half of the wing

According to Figure 5, displacement of q_0 is measured relative to reference coordinates and displacements of q_1 and q_2 are measured relative to elastic axis of the wing. Considering the above points, kinetic energy of the system will be as below:

$$T = \frac{1}{2}(m_0\dot{z}_0^2 + m_1\dot{z}_1^2 + m_2\dot{z}_2^2) \quad (21)$$

Given that $z_0=q$, $z_1=q_0+q_1$ and $z_2=q_0+q_2$, equation (2) after simplification will be as below:

$$T = \frac{1}{2}(m_T\dot{q}_0^2 + m_1\dot{q}_1^2 + 2m_1\dot{q}_1\dot{q}_0 + 2m_2\dot{q}_0\dot{q}_2 + m_2\dot{q}_2^2) \quad (22)$$

Where, $m_T=m_0+m_1+m_2$.

Potential energy of the system consists of two parts of potential energy resulted from gravity due to vertical displacement, U_g and potential energy resulted from internal strain, U_i. Strain potential energy will be equal to:

$$U_i = \frac{1}{2}\sum_{i=1}^{2}\sum_{j=1}^{2} k_{ij} q_i q_j = \frac{1}{2}(k_{11}q_1^2 + k_{12}q_1q_2 + k_{21}q_2q_1 + k_{22}q_2^2) \tag{23}$$

k_{ij} represents coefficients of effect which will be described below. Gravitational potential energy equals to:

$$U_g = -(P_{g0})q_0 - p_{g1}(q_0 + q_1) - P_{g2}(q_0 + q_2) \tag{24}$$

And aerodynamic forces will also be equal to:

$$Q_0 = P_{a0} + P_{a1} + P_{a2}\,, \quad Q_1 = P_{a1}\,, \quad Q_2 = P_{a2} \tag{25}$$

By obtaining partial derivative of equation (26) relative to $\dot{q}_0$ the following equation is obtained:

$$\frac{\partial T}{\partial \dot{q}_0} = m_T\dot{q}_0 + m_1\dot{q}_1 + m_2\dot{q}_2 \tag{26}$$

By obtaining the derivative of equation (27) relative to time, the following equation is obtained:

$$\frac{d}{dt}\left(\frac{\partial T}{\partial \dot{q}_0}\right) = m_T\ddot{q}_0 + m_1\ddot{q}_1 + m_2\ddot{q}_2 \tag{27}$$

Partial derivative of equations (28) and (29) relative to $\dot{q}_0$ are zero; but partial derivative of equation (5) is equal to:

$$\frac{\partial U_g}{\partial q_0} = -(P_{g0} + P_{g1} + P_{g2}) \tag{28}$$

By placing equations (26), (27) and (28) in Lagrange equation, the following equation is obtained:

$$\begin{aligned} m_T\ddot{q}_0 + m_1\ddot{q}_1 + m_2\ddot{q}_2 &= P_{a0} + P_{g0} + P_{a1} + P_{g1} + P_{a2} + P_{g2} \\ &= P_0 + P_1 + P_2 \end{aligned} \tag{29}$$

The same method is used in order to obtain the other two equations. Full description of obtaining the other equations is given in Reference (Warren Woodrow, 2013). The aerodynamic equations of the system are as below:

$$\begin{aligned} &m_T\ddot{q}_0 + m_1\ddot{q}_1 + m_2\ddot{q}_2 = P_0 + P_1 + P_2 \\ &m_1\ddot{q}_0 + m_1\ddot{q}_1 + k_{11}q_1 + k_{12}q_2 = P_1 \\ &m_2\ddot{q}_0 + m_2\ddot{q}_2 + k_{21}q_1 + k_{22}q_2 = P_2 \end{aligned} \tag{30}$$

Equations (31) can also be shown in the following matrix form:

$$[m_{ij}]\{\dot{q}_i\} + [k_{ij}]\{q_j\} = \{Q_j\} \tag{31}$$

Where,

$$\{\ddot{q}_j\} = \begin{bmatrix} \ddot{q}_1 \\ \ddot{q}_2 \\ \vdots \\ \ddot{q}_n \end{bmatrix} \qquad \{q_j\} = \begin{bmatrix} q_1 \\ q_2 \\ \vdots \\ q_n \end{bmatrix} \qquad \{Q_j\} = \begin{bmatrix} Q_1 \\ Q_2 \\ \vdots \\ Q_3 \end{bmatrix}$$

$[m_{ij}]$ is inertia matrix and $[k_{ij}]$ is matrix of coefficients of effect. Matrix of coefficients of effect is equal to inverse of stiffness matrix $[C_{ij}]$. So,

$$[k_{ij}] = [C_{ij}]^{-1} \quad (32)$$

Members of stiffness matrix, $[C_{ij}]$ s, represent the deviation created at the point i due to the effect of unit load on the point $j.n$ also indicates the number of degrees of freedom of the system.

Obtaining natural frequencies of wing and body of the aircraft

Using the equations obtained in this section and structural information of passenger aircraft shown in appendix (1), the structure of this aircraft has been modeled as concentrated masses connected to each other by bending elements without mass according to Figure 6.

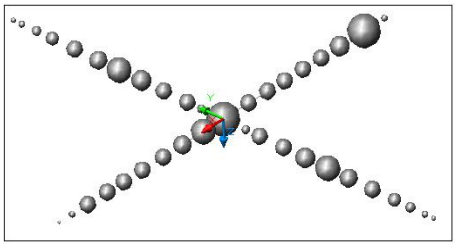

Figure 6. Concentrated mass model of aircraft

Information on masses and elements. Figure 5 shows the first natural vibrational frequency of aircraft wing. As it can be seen, by discretization of the wing into 3 concentrated masses, the calculated frequency is equal to 7.6 radians per second and with increasing of the number of masses, the calculated frequency is converged toward the real value. By considering 12 concentrated masses, the calculated frequency is equal to 13.2 radians per second.

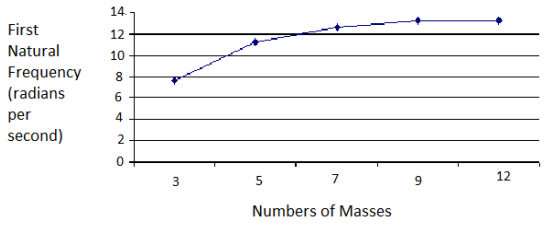

Figure 7. The first natural frequency of aircraft wing considering different numbers of masses

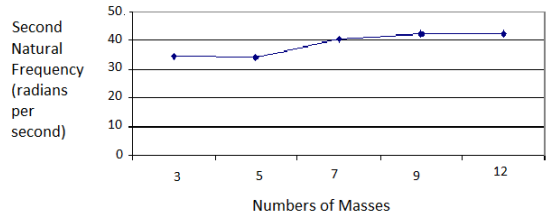

Figure 8. The second natural frequency of aircraft wing considering different numbers of masses

In Figures 9, 10 and 11, the second, third and fourth natural frequencies, respectively, calculated considering different numbers of concentrated masses have been shown. As can be seen in all these figures, as the number of concentrated masses increases, the calculated frequency becomes more accurate and converges toward real value.

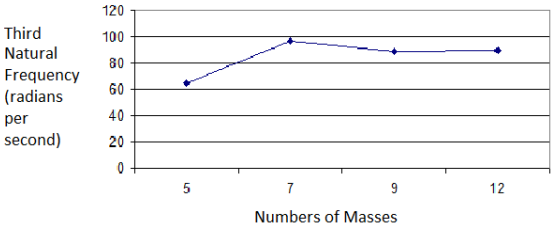

Figure 9. The third natural frequency of aircraft wing considering different numbers of masses

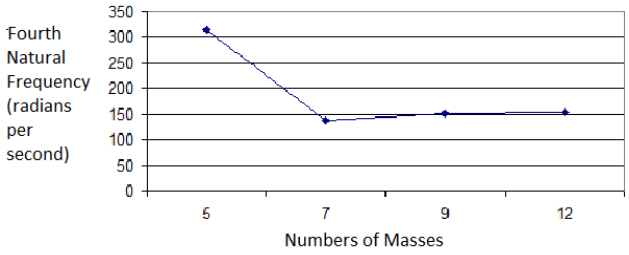

Figure 10. The fourth natural frequency of aircraft wing considering different numbers of masses

Summary of the results obtained for wing is shown in Table 2.

Table 2. Natural vibrational frequencies of aircraft wing considering different numbers of masses

Number of masses	The first frequency (Radian per second)	The second frequency (Radian per second)	The third frequency (Radian per second)	The fourth frequency (Radian per second)
3	7.6029	34.355	-	-
5	11.2	34.096	65.099	315.14
7	12.59	40.417	97.046	137.67
9	13.228	42.317	88.548	151.16
12	13.223	42.464	89.723	152.9

3. Results

Obtaining natural frequency of aircraft body

Similar to the previous section, using structural information of aircraft body and considering one-end closed beam model for the body such that the center of mass is the support and the end of the aircraft is the free end of the beam, and using the equations in the previous section, natural vibrational frequencies of body of the aircraft have been calculated. Similar to the results obtained for wing, it can be seen that as the number of masses increases, the obtained results converge toward real value. Figure 11 shows the first natural vibrational frequency of the body considering different numbers of concentrated masses.

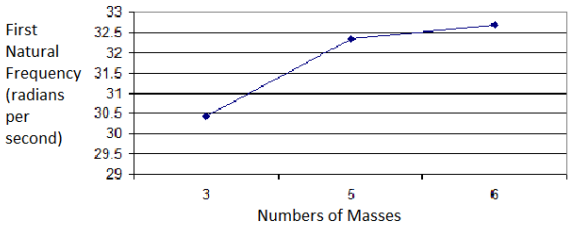

Figure 11. The first natural frequency of aircraft body considering different numbers of masses

By considering 3 concentrated masses, the calculated frequency is equal to 30.43 radians per second, and by considering 6 concentrated masses, this frequency is equal to 32.67 radians per second.

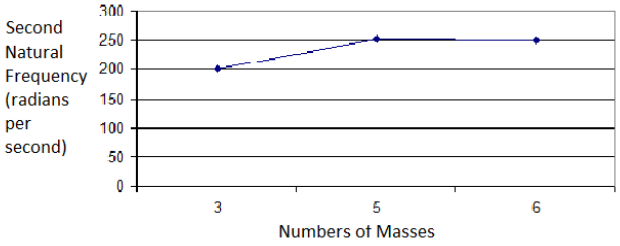

Figure 12. The second natural frequency of aircraft body considering different numbers of masses

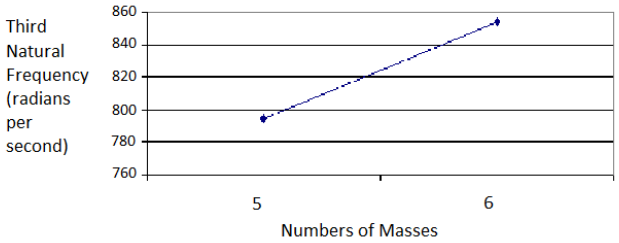

Figure 13. The third natural frequency of aircraft body considering different numbers of masses

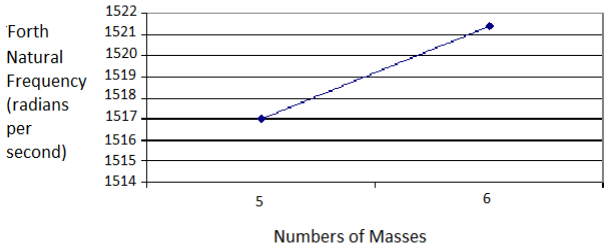

Figure 14. The fourth natural frequency of aircraft body considering different numbers of masses

Table 3. Natural vibrational frequencies of aircraft body considering different numbers of masses

Number of masses	**The first frequency (radian per second)**	**The second frequency (radian per second)**	**The third frequency (radian per second)**	**The fourth frequency (radian per second)**
3	30.434	199.97	-	-
5	32.332	252.07	794.66	1517
6	32.675	250.78	854.34	1521.4
Finite Element method	28.32	220.18	749.41	1120.23

Figures 11, 12, 13 and 14 show the second, third and fourth natural frequencies calculated in radians per second, respectively, for aircraft body considering different numbers of concentrated masses. As can be seen in all these graphs, as the number of concentrated masses increase, the calculated frequency converges toward the real value. The results obtained from calculation of natural frequencies of the aircraft body are shown in Table 3. Also, natural frequencies of the aircraft body have been calculated using Finite Element method, the obtained results of which show that the results obtained from the two methods are similar to each other. As the results of calculation of natural vibrational frequency of aircraft body show, the body of the aircraft has significant stiffness. In order to observe the effects of body flexibility on aircraft aerodynamics, these calculations have been done assuming increasing flexibility of body, similar to the case done in the third section, assuming increasing the flexibility 10 times, so that they obtained results can be used in flight simulation of elastic aircraft. The results of these calculations are shown in Figures 15 to 18.

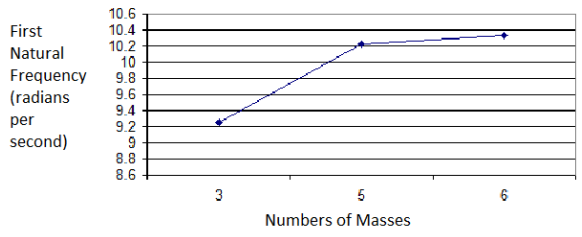

Figure 15. The first natural frequency of aircraft body considering different numbers of masses for highly elastic body

As can be seen, as the flexibility of body increases to the extent stated, a significant reduction in the aircraft's natural frequencies is created such that flexibility effects of the aircraft body on its aerodynamics cannot be ignored.

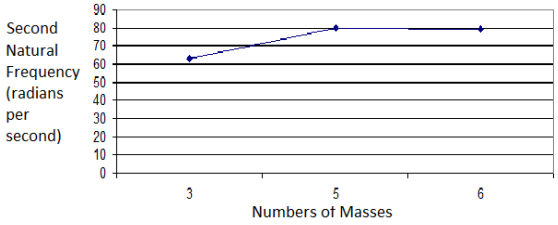

Figure 16. The second natural frequency of aircraft body considering different numbers of masses for highly elastic body

Figure 17. The third natural frequency of aircraft body considering different numbers of masses for highly elastic body

Figure 18. The fourth natural frequency of aircraft body considering different numbers of masses for highly elastic body

Also, the process of increasing accuracy of the calculated frequency can be observed in these forms similar to the previous cases.

Table 4. Natural vibrational frequencies of aircraft body considering different numbers of masses for highly elastic body

Number of masses	The first frequency (radian per second)	The second frequency (radian per second)	The third frequency (radian per second)	The fourth frequency (radian per second)
3	9.257	63.237	-	-
5	10.224	79.713	251.29	479.73
6	10.333	79.304	270.16	481.11

Summary of the results obtained in this section is shown in Table (4).

This section described how to obtain natural frequencies and shape of modes of continuous systems, and natural frequencies of aerodynamics of wing and body of passenger aircraft were calculated. The obtained results in this section will be used to simulate aircraft flight considering flexibility of its structure.

4. Conclusion

In this project, the effect of aircraft body flexibility in aerodynamic mode was studied. In the second section, assuming creation of bending in the body by horizontal and vertical tails, the longitudinal and transverse stability derivatives of the aircraft were obtained and, as shown, body flexibility reduced stability of the aircraft and also reduced power of tail control surfaces. This decrease increases with increasing speed such that these effects are noticeable at higher speeds. In the next section, natural frequencies of aircraft structure were obtained by discretization of continuous masses into discrete concentrated masses, and as observed, as the number of masses increased, the obtained

results became more accurate and converged toward real value. In investigations, passenger aircrafts have relatively high stiffness such that flexibility effect of body on aircraft cruise flight is not significant. However, if the plane is subjected to unplanned maneuver of plunging in critical conditions and given the fact that the aircraft has not been designed for such maneuvers, the impact of body flexibility in such conditions would be significant, that as was observed. So it is necessary to obtain airplane conversion function with regard to flexibility of the structure. In this case, the zeros and poles of elastic airplane conversion function will be different from stiff state and require specific measures.

REFERENCES

1. Chernyshev, L., Sergey Lyapunov, V., & Andrey, V. (2019). *Modern problems of aircraft aerodynamics*. Chernyshevet al., Advances in Aerodynamics, (2019) 1(7), 1-15. https://doi.org/10.1186/s42774-019-0007-6.
2. Cui, K., Xiao, Y., Xu, Y., & Li, G. (2018). *Hypersonic i-shaped aerodynamic configurations.* Science China Physics, Mechanics & Astronomy 619. 10.1007/s11433-017-9117-8.
3. Du, S., & Tang, Zh. (2018). *The Aerodynamic Behavioral Study of Tandem Fan Wing Configuration.* International Journal of Aerospace Engineering, Vol. 2018, Article ID 1594570, 1-14. https://doi.org/10.1155/2018/1594570.
4. Guttag, M., & Reis, P. M. (2017). *Active aerodynamic drag reduction onmorphable cylinders*. Physical Review Fluids 2(12). American Physical Societ. http://dx.doi.org/10.1103/PhysRevFluids.2.123903.
5. Heinz, S. (2017). *Aero elastic Concepts for Flexible Aircraft*. ISBN 978-91-7178-706-4.
6. Ideen, S. (2020). *Aerodynamic Design & Optimization*. Edition: 2.12, Publisher: CFD Open Series.
7. Li, Y. Q., Zheng, X., Teng, J., & You, Y. (2020). *Dual waverider concept for inlet-airframe integration with controllable wallpressure distribution.* In 21st AIAA international space Planes. Aerospace Science and Technology, 107, 106266. https://doi.org/10.1016/j.ast.2020.106266.
8. Naveen, R. (2018). *Aerodynamic Analysis of C-Wing Aircraft*. INCAS BULLETIN, 10(3), 157–165. DOI: 10.13111/2066-8201.2018.10.3.13.
9. Stalewski, W., & Żółtak, J. (2014). *Design of a turbulent wing for small aircraftusing multidisciplinary optimisation.* Arch. Mech. 66 (3), 185-201.
10. Tuzcu, I. (2016). *Dynamics and Control of Flexible Aircraft. Dissertation submitted to the faculty of the Virginia Polytechnic Institute and state university for the degree of Doctor of philosophy in Mechanical Engineering.* Virginia Tech, http://rightsstatements.org/ vocab/InC/1.0/.
11. Warren Woodrow, H. (2013). *Aircraft Design Optimization as a Geometric Program.* Adissertation submitted in partial satisfaction oft herequirements for the degree of Doctor of Philosophy, University of California, Berkeley. http://web.mit.edu/~whoburg/www/ papers/hoburg_phd_thesis.pdf.
12. Xianhong, X., Yuan, L., & Qian, Z. (2017). *Investigation of a wide range adaptable hypersonic dual-waverider integrativedesign method based on two different types of 3d inward-turning inlets*. In 21st AIAA international space Planes,hypersonic systems and technologies conference. https://doi.org/10.2514/6.2017-2110.

Mohammad Reza HASSANNEZHAD - B. Sc. of Aeromechanic Technology Engineering, Aviation Services and Technology University of Applied Science of Mashhad, Iran. His favorite topics include: space mechanics, mechanical physics, aerospace and other topics related to this field.